

THE DOUBLE CAPSTAN AS A POSITION CONTROLLER

by

JANET ELIZABETH FREEMAN


SUBMITTED IN PARTIAL FULFILLMENT
OF THE REQUIREMENTS FOR THE
DEGREE OF

BACHELOR OF SCIENCE

at the

MASSACHUSETTS INSTITUTE OF TECHNOLOGY

May 19, 1978

Signature of Author 
Department of Mechanical Engineering, May 19, 1978

Certified by 
Thesis Supervisor

Accepted by 
Chairman, Departmental Committee on Thesis

Archives
MASSACHUSETTS INSTITUTE
OF TECHNOLOGY

JUL 10 1978

LIBRARIES

THE DOUBLE CAPSTAN AS A POSITION CONTROLLER

by

JANET ELIZABETH FREEMAN

Submitted to the Department of Mechanical Engineering on May 19, 1978 in partial fulfillment of the requirements for the Degree of Bachelor of Science.

ABSTRACT

The double capstan controller amplifies force signals that are created by a displacement input. A second-generation model was built and found to behave as a second-order position control system. Its natural frequency is 7.64 cps, low-frequency gain is 4.17, and damping ratio 0.40. The theoretical model predicts the natural frequency within 5%, the gain within 14%, and the damping ratio within 12%. The actual gain and damping ratio are different from predictions because the input lever for the system was hitting stops at resonance. The physical limits on input lever motion caused actual gain to be lower and damping ratio to be higher than they would be if the lever were not limited in its travel.

Thesis Supervisor: Woodie C. Flowers
Title: Associate Professor of Mechanical Engineering

ACKNOWLEDGEMENTS

This project has been an incredible learning experience because of the time and patience of many other people. The construction of the model would have been impossible without the help of Sam, Tiny, Ray, Bill, Frank and Fred in the three Mechanical Engineering machine shops. The Electrical Engineering department's 5th floor student lab kindly allowed me to use their space and electronic equipment for measurements. Doug White was generous with his time, trouble-shooting skills, equipment, and sympathy when he had many other projects to finish. My advisor Professor Woodie Flowers and Undergraduate Secretary/typist Peggy Garlick are two very understanding people. To these and all others whose knowledge and kindness helped me through this experience, I am deeply grateful.

My special thanks goes to Peter Cunningham, my fiance, who lovingly shared in all aspects of this project. We both learned from it.

TABLE OF CONTENTS

	<u>PAGE</u>
ABSTRACT	2
ACKNOWLEDGEMENTS	3
LIST OF FIGURES	5
I. INTRODUCTION	6
II. THEORETICAL ANALYSIS	9
2.1. The Double Capstan	9
2.2. The Input Lever	12
2.3. Motion of a Mass	14
2.4. Block Diagram	15
2.5. Design Tradeoffs	18
III. DESIGN OF THE MODEL	21
IV. EXPERIMENTAL PROCEDURE	27
4.1. Capstan Gain	27
4.2. System Response to Sinusoidal Input	29
V. RESULTS AND DISCUSSION	31
5.1. Capstan Gain	31
5.2. System Dynamic Response	32
VI. CONCLUSIONS AND RECOMMENDATIONS	36

LIST OF FIGURES

<u>FIGURES</u>		<u>PAGE</u>
1	Amputee Controlling Overhead Cart with the Proposed Double Capstan System.	7
2	Tensions in a Rope Wrapped around a Capstan.	10
3	Tensions in Ropes Wrapped around Double Capstan.	10
4	Input Lever Schematic (Overhead View).	13
5	Mass-Dashpot Model of Mass Attached to Double Capstan.	13
6	Block Diagram without Feedback.	17
7	Block Diagram with Feedback.	17
8	The Second-Generation Double Capstan Controller System.	22
9	Input Lever	26
10	Schematic of Set-Up for Determining Capstan Gain.	28
11	The Sinusoidal Input Mechanism (Schematic).	28
12	Bode Magnitude Plot of System Response to Sinusoidal Input.	33

I. INTRODUCTION.

The double-capstan controller was first suggested by M.I.T. Professor Woodie C. Flowers and Alvin G. Dulcan, Jr., as a possible solution to a particular design problem. The MIT Knee Group needed a way to make a previously-built cart follow an above-knee amputee as the person walked using an experimental knee prosthesis. The cart ran in a track on the ceiling, and supported short but heavy electrical and hydraulic cables that connected to the prosthesis. The cart did not move easily; having to pull the cables and cart along while walking interfered with the amputee's natural gait, which could have resulted in erroneous experimental data.

The proposed double-capstan system required only a small movement, with little accompanying physical effort from the operator, to move a cart attached to the double capstan (Figure 1). In this system, a small force input was amplified to create a large force capable of moving "heavy loads". A small input displacement created the input force by stretching a spring. The double capstan was thus controlled by displacement input and feedback. An amputee using the double capstan attached to the heavy cart could thereby control the cart

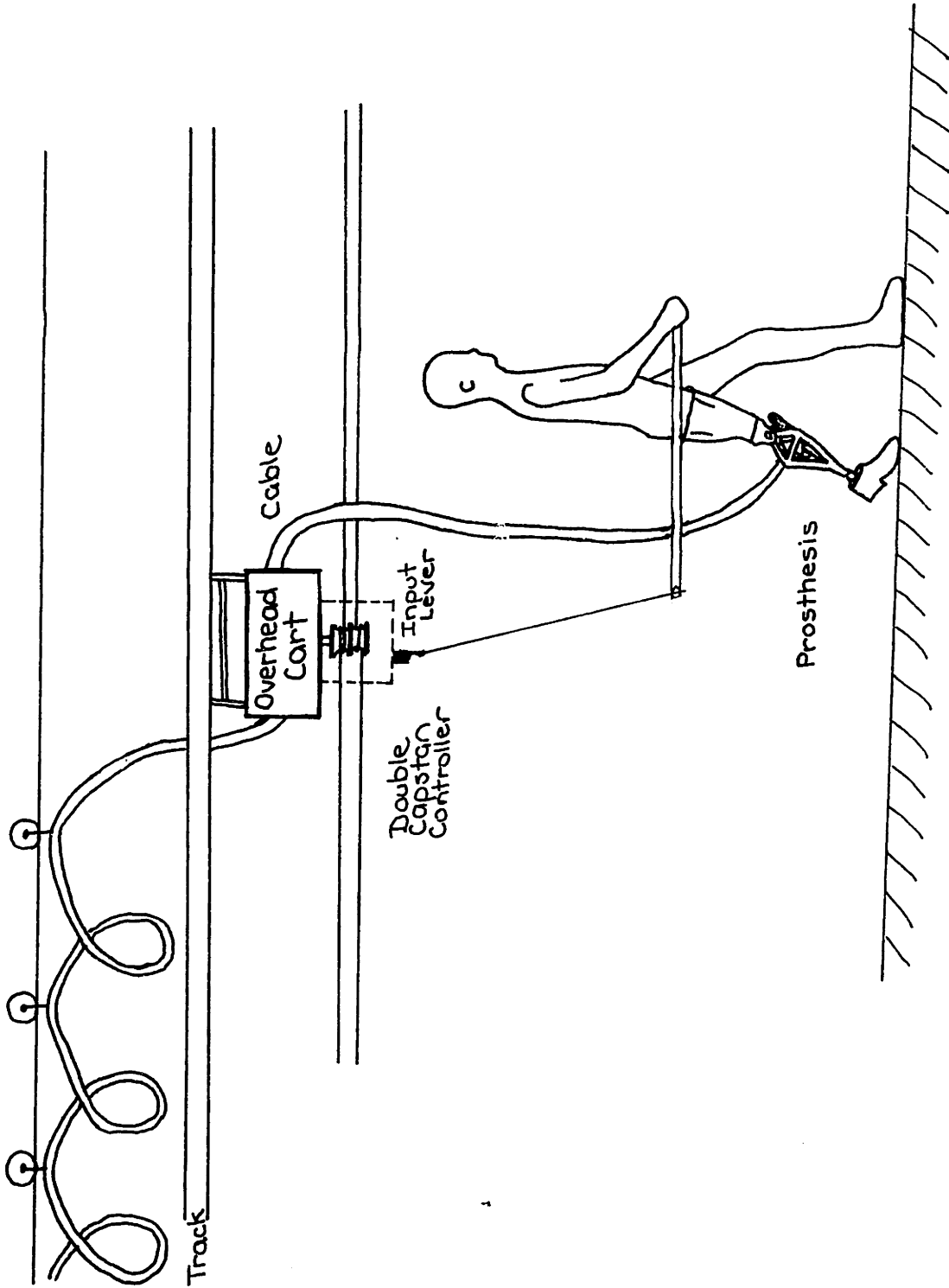


Figure 1. Amputee Controlling Overhead Cart with the Proposed Double Capstan System.

through small, virtually effortless movements. Gait would be unaffected.

Dulcan built a small model of a double-capstan controller and studied its properties (MIT Mechanical Engineering S.B. Thesis, 1974). He found his system to be simple and useful, but unfortunately not predictable. He had planned to use a second-order dynamic model to represent the system; however, tests indicated the system was greater than fourth order. Some of the differences between results and theory were attributed to design and construction of that particular model. Other differences could not be explained. Dulcan suggested a mathematical dynamic model be developed as the next step.

This thesis involves design, construction, and theoretical modelling of a second double-capstan controller system. Although the need to control the overhead cart for prosthetics experiments has since been filled by another device, the double capstan can still be useful in other applications where simple position control is required.

II. THEORETICAL ANALYSIS

Equations for the double-capstan controller system can be developed by first finding individual relations for the double capstan, the input lever, and the motion of the mass attached to the double capstan. These relations can be incorporated into a block diagram with feedback. Equations predicting dynamic behavior can then be found from the diagram. Design tradeoffs can also be explained in terms of the individual relations.

2.1. The Double Capstan

A capstan acts as a mechanical force amplifier when spinning. A rope wrapped around an unmoving capstan will have the same tension at both ends. The tensions in the two ends will differ, however, when the capstan is spinning. Friction acts between the rope and the rotating capstan to create a drag which pulls on one end of the rope and slacks the other end. The ratio of the higher tension T_H to the lower tension T_L depends on the coefficient of friction, f , and the angle of contact, θ :

$$T_H = T_L e^{f\theta}. \quad (1)$$

Figure 2 shows a capstan with one loop of rope around it, so that $\theta = 2\pi$. Gain should not vary with capstan speed if f and θ are constant.

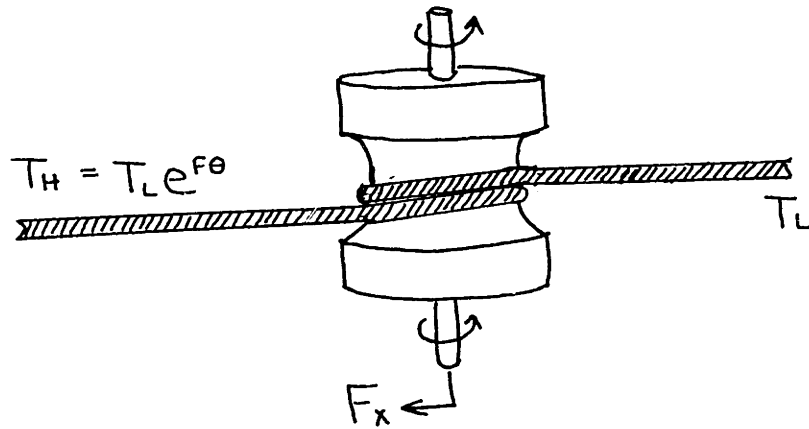


Figure 2. Tensions in a Rope Wrapped around a Capstan.

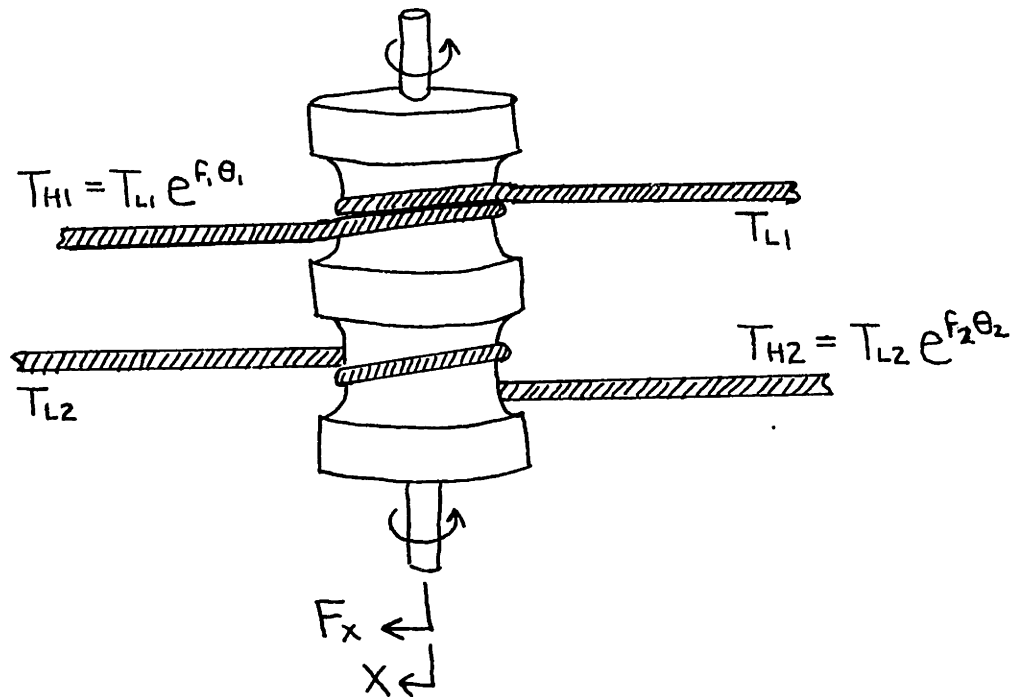


Figure 3. Tensions in Ropes Wrapped around a Double Capstan.

Two capstans machined onto one continuous piece of material are the double capstan. If a rope is wrapped around one of the capstans while the double capstan is spinning, there will be a force imbalance acting on the double capstan of magnitude

$$\begin{aligned} F_x &= T_H - T_L \\ &= T_L (e^{f\theta} - 1). \end{aligned} \quad (2)$$

If a second rope is wrapped around the second capstan so that its low tension end is on the same side of the double capstan as the high tension end of the first rope (Figure 3), the force acting on the double capstan is:

$$\begin{aligned} F_x &= (T_{H1} + T_{L2}) - (T_{L1} + T_{H2}) \\ &= (T_{L1} e^{f_1\theta_1} + T_{L2}) - (T_{L1} + T_{L2} e^{f_2\theta_2}) \end{aligned} \quad (3)$$

If the coefficient of friction and the angle of wrap are the same for both capstan, equation 3 becomes

$$F_x = (T_{L1} - T_{L2}) (e^{f\theta} - 1). \quad (4)$$

When the two low tensions are equal, the net force F_x is zero. However, if a small difference exists between the two low tensions, the net force F_x is not zero,

but instead is the difference in low tensions multiplied by a gain term. This amplified force can be used to move the double capstan and objects attached to it. The advantage of the double over a single capstan for amplifying force is that F_x on the double capstan can be made to act in two directions. Note, however, that the two ropes constrain the capstan to motion along a straight line.

2.2. The Input Lever

The input lever creates the difference between tensions T_{L1} and T_{L2} that is needed to create the net force F_x . A schematic of the input lever's function is shown in Figure 4. The input lever is connected to the low-tension ends of the two ropes wrapped around the capstan. When the lever is moved by an input displacement, it pulls on one low-tension rope and slacks the other. The ropes are assumed not to stretch. Because the rope cannot stretch or relax, the input displacement is taken up directly by the two springs. Each spring is assumed to have an initial displacement so that each can shorten by the amount of the input displacement without reaching its unstretched length.

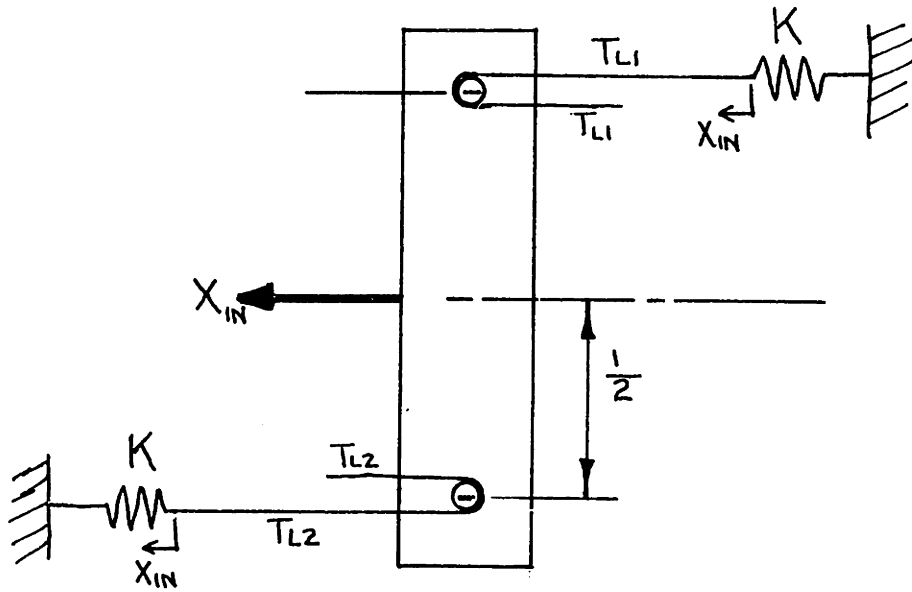


Figure 4. Input Lever Schematic (Overhead View).

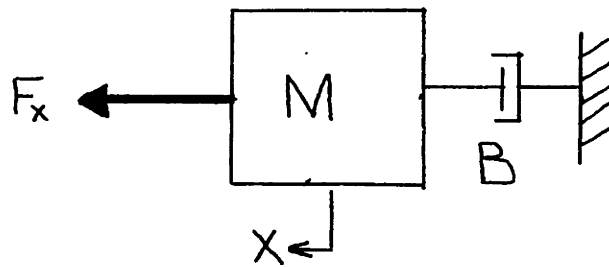


Figure 5. Mass-Dashpot Model of Mass Attached to Double Capstan.

Let each spring have an equal spring constant K . Also, let the input displacement change the force by the amount ΔT , where

$$\Delta T = KX_{in} . \quad (5)$$

Let the initial displacement length of each spring be the same, so that T_L is the initial tension in each rope. Then for an input X_{in} in the direction shown,

$$T_{L1} = T_L + \Delta T \quad (6)$$

$$T_{L2} = T_L - \Delta T$$

The difference in the low tensions of the ropes can now be expressed in terms of an input displacement:

$$\begin{aligned} T_{L1} - T_{L2} &= (T_L + \Delta T) - (T_L - \Delta T) \\ &= 2\Delta T \\ &= 2KX_{in} . \end{aligned} \quad (7)$$

2.3. Motion of a Mass

The force-amplification property of the double capstan can be put to use by attaching the double capstan to some heavy object to be moved. A small force input to a low tension of the double capstan system could create a force large enough to move the object if system parameters are chosen carefully.

The motion of the mass with the double capstan system attached can be found from the mass-dashpot schematic in Figure 5. The input force F_x must overcome the inertia of the mass and the resistance of the bearings (represented by the dashpot B) to move the mass in the x-direction.

The linear equation for this arrangement is

$$M\ddot{x} + B\dot{x} = F_x. \quad (8)$$

Define an operator s , such that

$$s = \frac{d}{dt}. \quad (9)$$

Then equation 8 becomes

$$Ms^2x + Bsx = F_x \quad (10)$$

$$\frac{x}{F_x} = \frac{1}{Ms^2 + Bs}. \quad (11)$$

2.4. Block Diagram

Equations 4, 7, and 10 form an overlapping set of equations:

$$(Ms^2 + Bs)x = F_x$$

$$F_x = (T_{L1} - T_{L2})(e^{f\theta} - 1)$$

$$T_{L1} - T_{L2} = 2Kx_{in}$$

The block diagram form of these equations appears in Figure 6.

The controller aspect of the double capstan can now be added. The input displacement actually depends in part on the position of the mass. The system should only receive input if the cart is not positioned as wanted.

To reflect this, feedback must be added to the block diagram. This is done in Figure 7. Because position output is being summed to a position input, only a gain of one is needed in the feedback loop.

The equations describing the motion of the system can be found from the block diagram:

$$\frac{X}{X_{in}} = \frac{2K(e^{f\theta} - 1)}{Ms^2 + Bs + 2K(e^{f\theta} - 1)} \quad (12)$$

ω_n = natural frequency

$$= \sqrt{\frac{2K(e^{f\theta} - 1)}{M}} \quad (13)$$

ξ = damping ratio

$$= \frac{B}{\sqrt{8MK(e^{f\theta} - 1)}} \quad (14)$$

G = gain

$$= 2K(e^{f\theta} - 1) \quad (15)$$

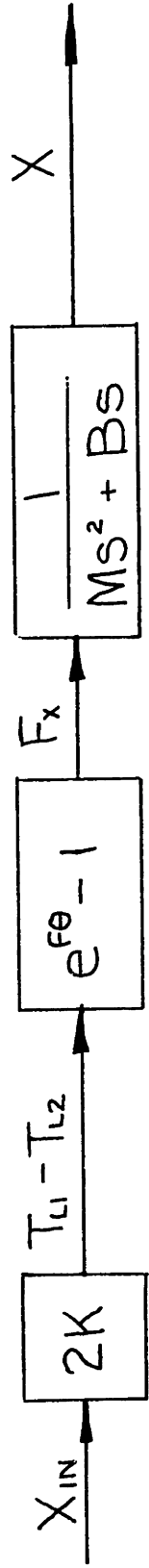


Figure 6. Block Diagram without Feedback.

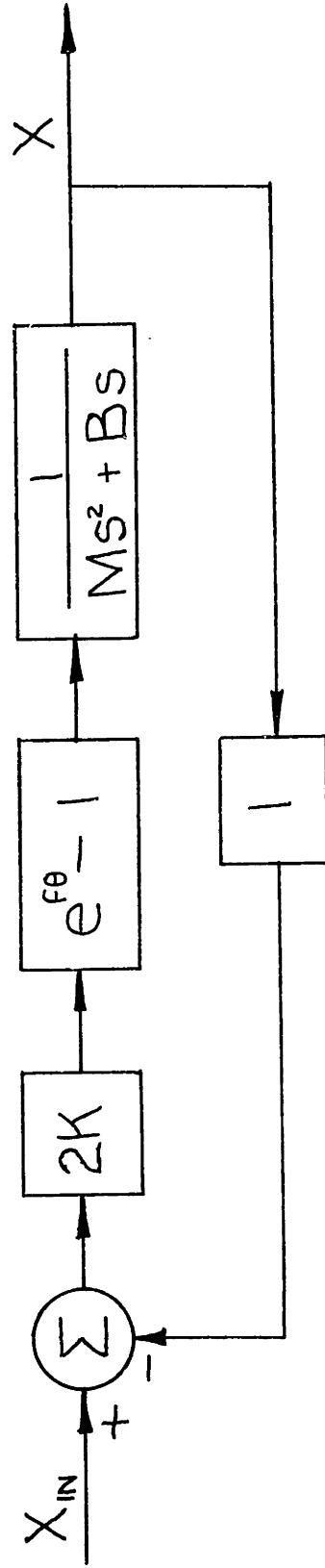


Figure 7. Block Diagram with Feedback.

2.5. Design Tradeoffs

Four important parameters in the system are influenced by rope tensions:

1. Force F_x acting on mass;
2. Force F_L needed to displace input lever;
3. Torque M_L acting to distort input lever, and
4. Power P dissipated at string-capstan interface.

The force F_x is proportional to the input tension ΔT and the gain:

$$F_x = 2\Delta T(e^{f\theta} - 1) \quad (16)$$

From Figure 4, the force to move the input lever is also proportional to ΔT :

$$\begin{aligned} F_L &= 2T_{L1} - 2T_{L2} \\ &= 2(T_L + \Delta T) - 2(T_L - \Delta T) \\ &= 4\Delta T . \end{aligned} \quad (17)$$

F_x must be large to move the cart. If F_x is made large by having ΔT large, however, the value of the amplifier is lost. It will take almost as much effort to move the input lever as it would to move the mass itself. Thus gain should be increased for larger masses.

To keep ΔT small, the spring K should be chosen carefully for the F_x desired.

Torque M_L on the input lever and power dissipation P from friction between the capstan and string are both proportional to the initial low tensions T_L . If the distance between the two posts on the lever is L , then from Figure 4 M_L is found to be

$$\begin{aligned} M_L &= \frac{L}{2} 2T_{L1} + \frac{L}{2} 2T_{L2} \\ &= L (T_L + \Delta T + T_L - \Delta T) \\ &= 2LT_L \end{aligned} \quad (18)$$

Power dissipated from a cord on a spinning cylinder is found from

$$P \propto R(T_H - T_L) \quad (\propto \equiv \text{proportional to})$$

$$P = P_{\text{top capstan}} + P_{\text{bottom capstan}}$$

$$P \propto R (T_{H1} - T_{L1}) + R (T_{H2} - T_{L2})$$

where R = radius of cylinder (capstan radius).

This reduces to

$$\begin{aligned} P &\propto R \left[T_{L1} (e^{f\theta} - 1) + T_{L2} (e^{f\theta} - 1) \right] \\ &\propto R (e^{f\theta} - 1) (T_L + \Delta T + T_L - \Delta T) \\ &\propto R (e^{f\theta} - 1) 2T_L \end{aligned} \quad (19)$$

Thus T_L must be low to reduce the torque acting on the input lever and to reduce the horsepower required of the motor used to drive the capstan. The radius of the capstan should be small to reduce both P and M_L . (The distance L between posts is set by capstan radius-see Design of Model.) But if gain $(e^{f\theta} - 1)$ must be maximized to move the cart, power losses will be affected as well.

It should also be noted that changing the gain $e^{f\theta}$ or spring constant K affects the natural frequency and damping ratio of the system. A larger gain is needed to move larger masses. Yet a large gain with a large mass could cause the damping ratio ξ to be extremely small if bearing damping B is not adjusted.

III. DESIGN OF THE MODEL

Figure 8 is comprised of pictures of the double-capstan system built for this thesis. A 3-lb. cart machined from a section of aluminum I-beam is the mass to be moved by the double capstan. Each of the 4 legs of the cart is connected to a plastic bearing which fits on rectangular steel rail. The coefficient of friction for the plastic bearings on the steel rail is 0.174. The cart runs on two rails supported by thin I-beam sections and by two large wooden blocks, one on each end of the track.

The output shaft of a DC permanent magnet motor protrudes from the bed of the cart at a 90° angle. The double-capstan (radius = 0.344") is attached to this shaft with set screws. Testing showed the horsepower of the motor was too small to withstand the drag of the string needed at cart motion, however. For this reason, a 1/4 hp variable speed drill was used to drive the capstan with a flexible shaft. The drill and flexible shaft are not shown in the pictures.

The strings that wrap around the double capstan are fastened at each end to hooks screwed into the wooden end blocks. The spring constant of the string used was estimated to be $35 \text{ lb}_f/\text{in.}$ for a 2 ft. length of string.

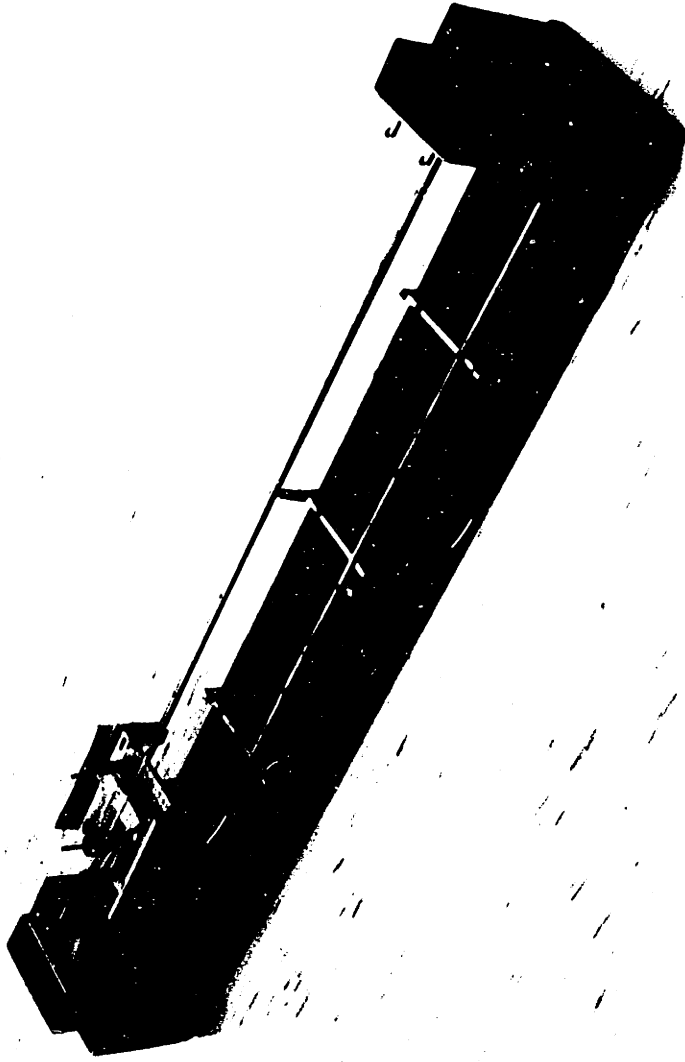


Figure 8a. The Second-Generation Double-Capstan Controller System.

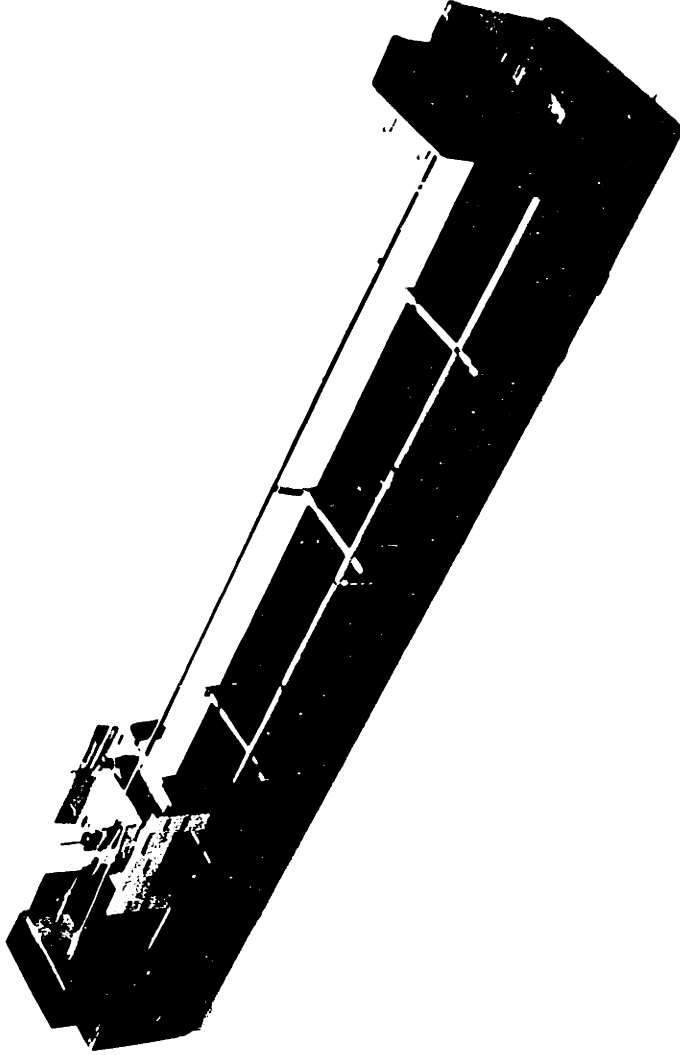


Figure 8a. The Second-Generation Double-Capstan Controller System.

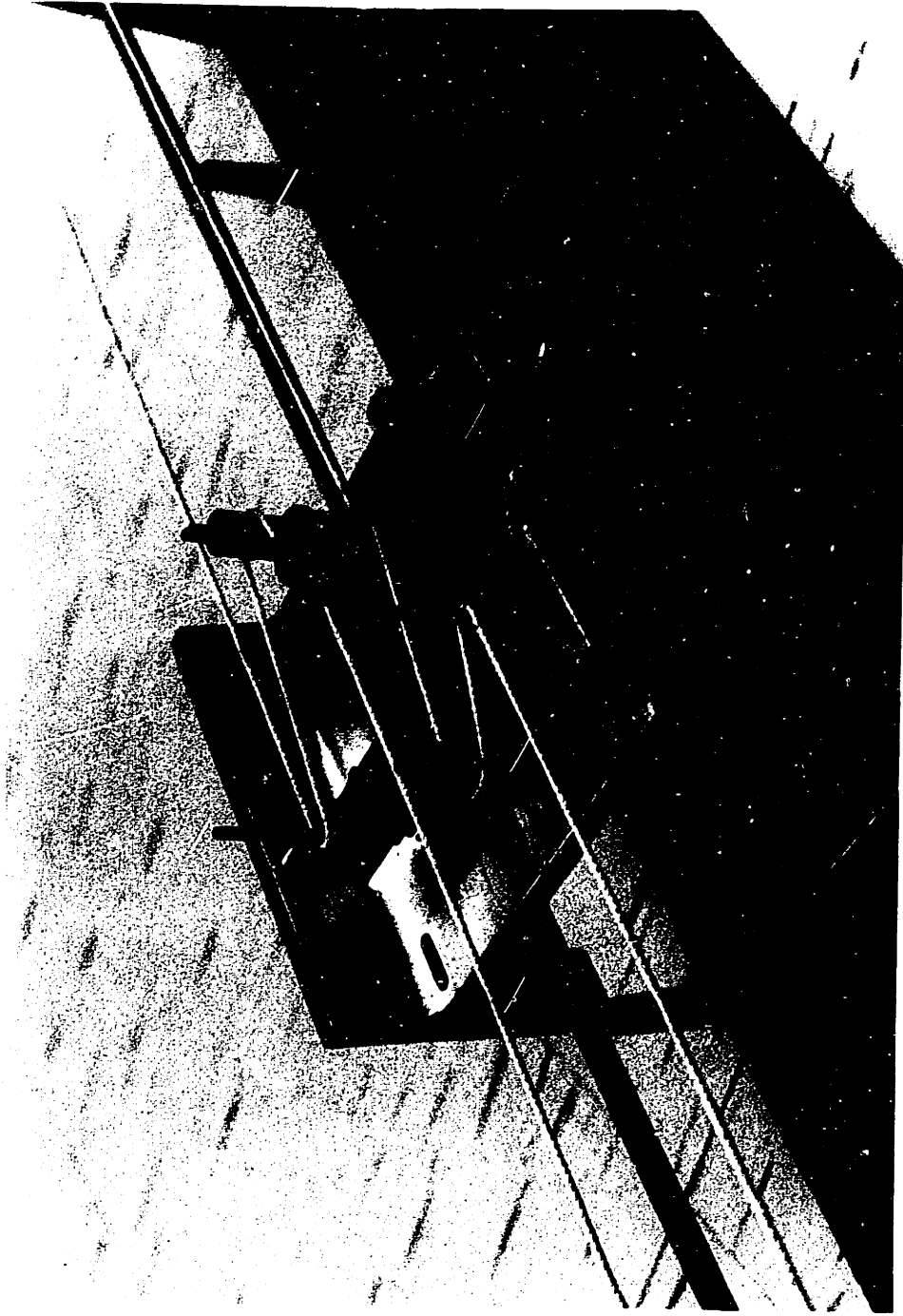


Figure 8b. The Second-Generation System.

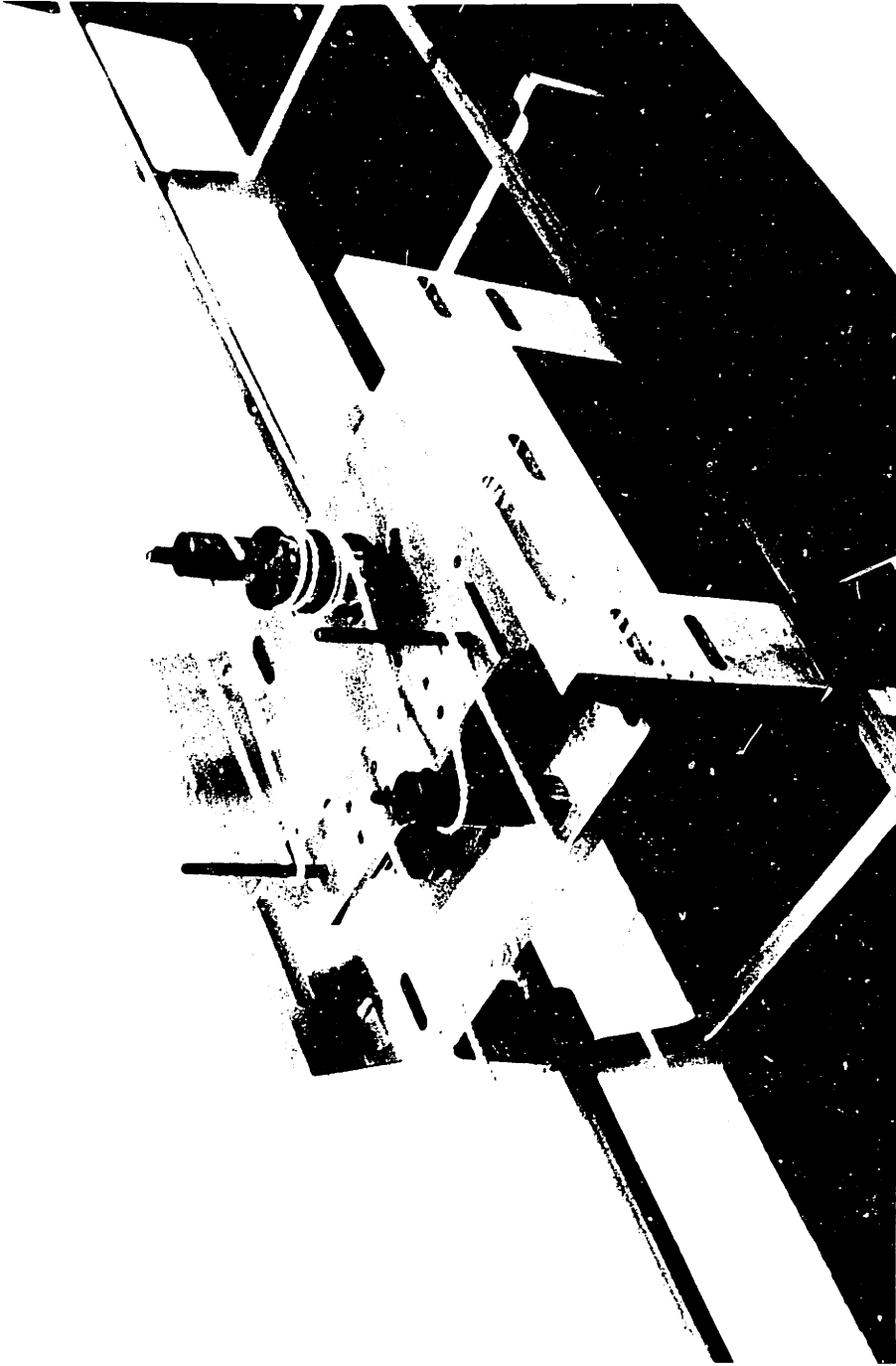


Figure 8b. The Second-Generation System.



Figure 8c. The Second-Generation System.

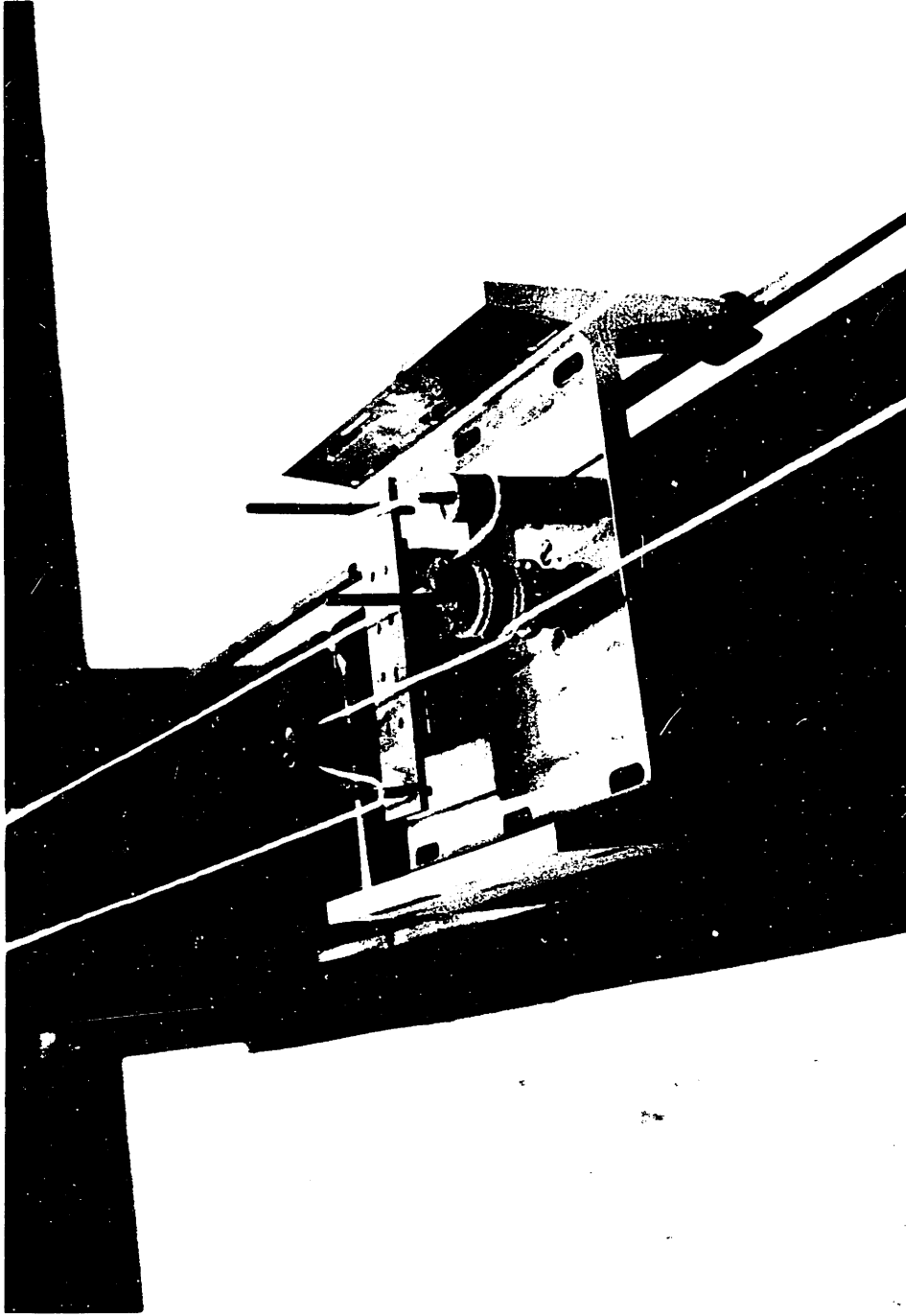


Figure 8c. The Second-Generation System.

Each string is threaded around posts on the input lever, as shown in Figure 9. The lever is attached to the cart with a flexure made of cabinet hinges. The hinges are used to prevent the lever arm from cocking, and to insure that each post is displaced by the same amount as the input lever. The resistance of the input lever to motion relative to the stationary cart is much smaller than the friction resisting cart motion along the rails.

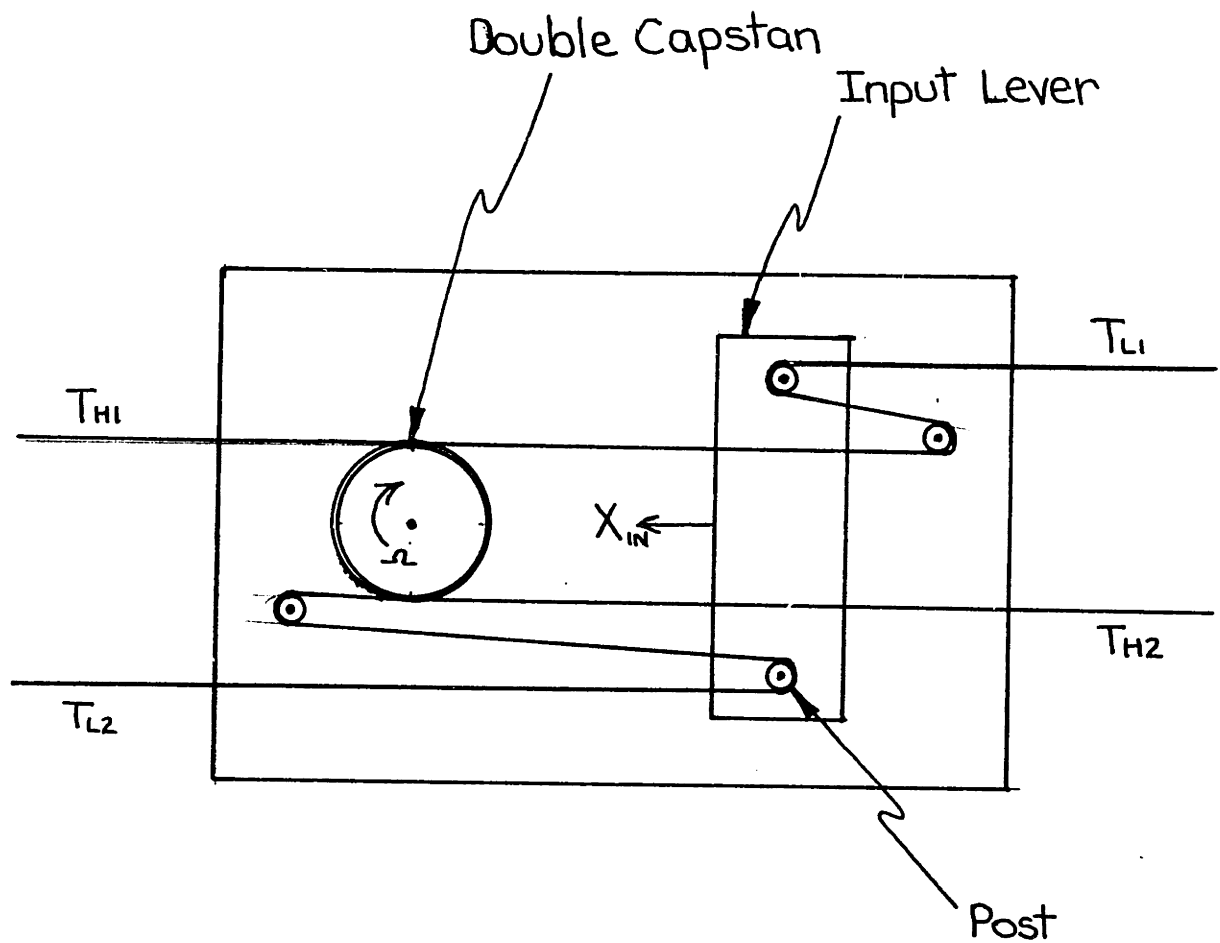


Figure 9. The Input Lever. movement in the X_{IN} direction increases T_{L1} , decreases T_{L2} .

IV. EXPERIMENTAL PROCEDURE

The behavior of the actual double-capstan controller was evaluated through two experiments: capstan gain, and the dynamic response of the controller to a sinusoidal input.

4.1. Capstan Gain

Two separate methods were used to empirically determine capstan gain. The gain is here taken to mean $T_H/T_L (=e^{f\theta})$. In one test, the motor was clamped to a workbench with the capstan left free to rotate. The string was draped over the capstan ($\theta = \pi$) and a known weight was placed on the low tension free end. The drill motor was then energized. A spring gage attached to the high tension end registered the T_H corresponding to the weight on T_L (Figure 10). This test was also done with $\theta = 3\pi$.

The second method tested the gain for the assembled system-- double capstan, input lever, and cart on the track. The strings were arranged as they would be when the system was running. Both $\theta = 2\pi$ and $\theta = 4\pi$ were tested. The cart was clamped, and the input lever secured so that neither moved. A leaf spring gage was placed on the low tension side of one string; another identical gage was placed on the corresponding high tension. Position

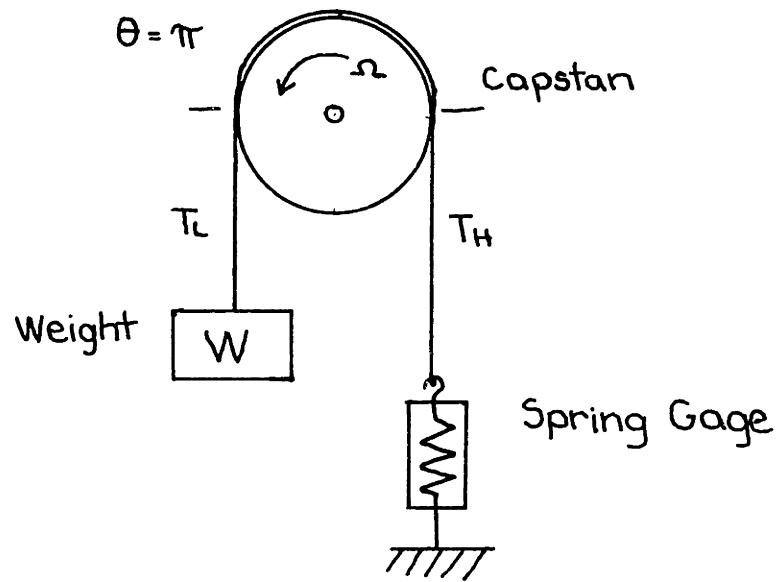


Figure 10. One Set-Up for Measuring Gain.

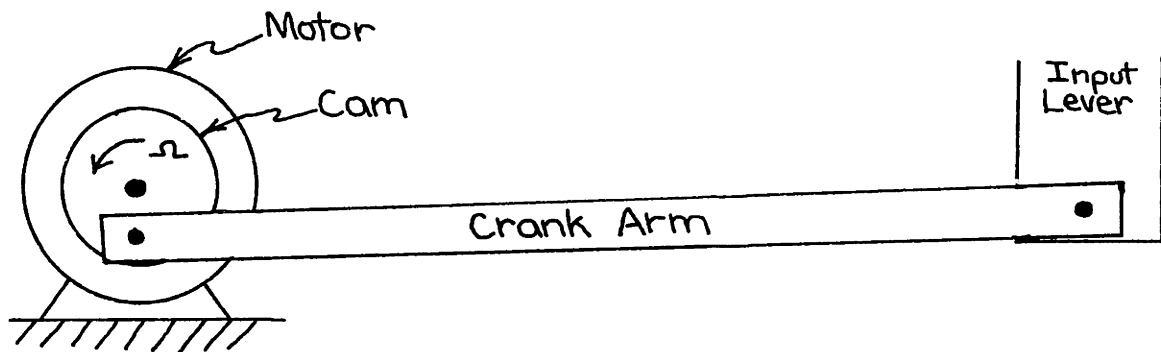


Figure 11. The Sinusoidal Input Mechanism (Schematic).

of the gages was adjusted so that each registered the same force while the capstan was stationary. The capstan was then energized, and the new readings on each gage were recorded. This was repeated with different initial tensions.

Both methods of determining gain were repeated with different capstan velocities. Both strings to be used on the cart were tested on their respective halves of the double capstan.

4.2. System Response to Sinusoidal Input

A sinusoidal input was generated by a DC gear-head motor with a circular cam attached. A crank arm pivoted about a screw fastened in the cam (Figure 11). The other end of the crank arm was connected by a pivot screw to the input lever. The crank arm was long enough that the circular motion of the cam end of the crank arm resulted in straight line motion of the input lever end. The motor remained stationary while the crank was running. To reduce the input frequency, motor speed was reduced by lowering the voltage to the motor. The input motor was turned on first, then the drill which drove the capstan was turned on. The drill was run at full speed for all tests.

The cart's response to this sinusoidal input was measured electrically. A copper wire attached to the cart slid along a length of high-resistance nichrome wire, which had a voltage placed across its ends. The voltage between one end of the wire and the copper wiper attached to the cart was fed through an amplifier. The amplifier output was displayed on a strip chart recorder. Amplitude and frequency were determined from this output. After each test, the chart recorder pen displacement in millimeters was calibrated in terms of cart displacement in inches.

V. RESULTS AND DISCUSSION

5.1. Capstan Gain

Capstan gain T_H/T_L averaged 3.75 when the angle of contact θ equalled 4π (two turns of string around the capstan), corresponding to a frictional coefficient f of 0.11. The range of values varied as much as 16% from this mean. Average gain for $\theta = 2\pi$ was 1.41 corresponding to an f of 0.05, with maximum 21% error in values. These results are for one capstan speed only.

The variations in gain when capstan speed is constant arise from the variation in T_L used to take data. Theoretically, $T_H/T_L = e^{f\theta}$ does not vary with T_L . In reality, however, when T_L is low, the string does not keep constant contact with the capstan surface. This varies θ , which in turn varies gain. This effect is indirectly responsible for the different gain values for the two values of θ . The same length of string was used for both tests. Although the securing hooks were adjusted as much as possible to reduce the length of string required, the string still had to be stretched a little to make 2 turns around the capstan. Thus initial tensions were higher for the $\theta = 4\pi$ gain tests, and

contact with the capstan was therefore more consistent and closer to theory. This is confirmed by the coefficients of friction derived from the gain. The $\theta = 4\pi$ value of $f = 0.11$ is closer to what would be expected of cotton twine on brass.

The capstan gain was found to decrease, however, as capstan speed decreased. This result is also not predicted by theory.

A possible cause is temperature effects on the string and the capstan. The capstan surface becomes too warm to touch after long use; the temperature might effect the string/capstan interface in some way. A thorough analysis of this result requires further study.

5.2. System Dynamic Response

The magnitude portion of a Bode plot appears in Figure 12. The shape of the curve indicates an underdamped second-order system.

The -40 dB/decade falloff is that of a second-order system. The asymptote of this falloff intersects the gain asymptote at the natural frequency of 48 rad/sec (7.64 cps). Equation 13 theoretically predicts a natural frequency of 45 rad/sec for measured parameter values of $M = 3$ lb_f/g , $K = 35$ lb_f/ft, and $e^{f\theta} = 3.75$. The 5% error is due to the assumption of constant K.

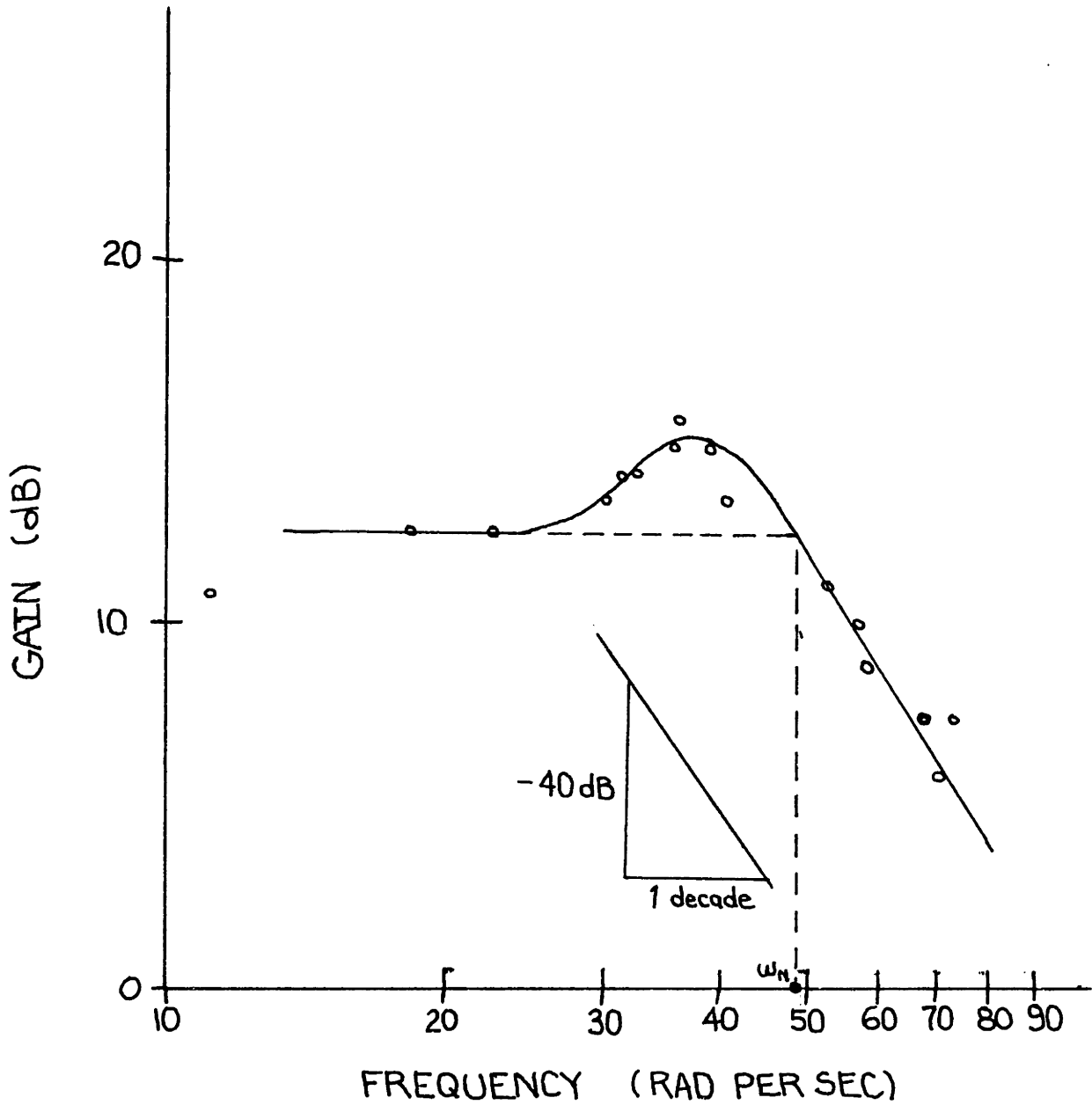


Figure 12. Bode Magnitude Plot of System Response to Sinusoidal Input.

The strings providing tension also serve as the springs, and the length of low-tension string varies with cart position for each capstan. Since the spring constant K of the string is a function of length, K will vary with cart position. The theoretical value is acceptably close to empirical value for prediction purposes.

Theory (equation 14) predicts a damping ratio of $\xi = 0.35$ for a measured B of 3.13 $\text{lb}_f\text{-sec/ft}$. (This value is actually the constant frictional force resisting motion regardless of velocity.) However, the height of the resonant peak indicates $\xi = .40$. This difference is a result of cart design. The input lever travel relative to the cart is limited. During testing, the sound of the lever hitting the stops was audible when the cart frequency was around ω_n . This indicates that gain would have been higher at resonance and that the damping ratio would be lower if there had been no physical limits on cart motion relative to the lever arm. This is a nonlinearity which is not represented in the proposed model. It also causes the resonant peak to appear to occur at a frequency smaller than ω_n .

The gain at low frequencies is 12.4 dB. Theoretical gain (equation 15) predicts gain at low frequencies to be 45.69 dB. This discrepancy is possibly a result of input lever design. However, if the K term is dropped from the theoretical gain (equation 15) then

$$G = 2 (e^{f\theta} - 1). \quad (20)$$

This predicts a low-frequency gain of 14.8 dB, which is much closer to the gain value obtained by experiments. The difference between this value and the actual value is 14%. Perhaps the K term may be dropped because the string does not act like a spring when cart motion is slow. This should be investigated further.

VI. CONCLUSIONS AND RECOMMENDATIONS

The physical model acts as a second-order position controller. The theoretical model is useful in predicting this behavior. Low-frequency gain predictions should be made from

$$\text{gain} = 2 (e^{f\theta} - 1) ,$$

which drops the K term from the theoretical gain in equation 15. The K term must be dropped for this particular device only. The actual values of the low-frequency gain and damping ratio will be much closer to predicted values when the length of travel of the input lever is increased. There is no reason to expect significant errors in these values once the limits are removed.

The gain of $e^{f\theta}$ between string tensions is not independent of initial string tension or capstan velocity. This dependence should be studied.

The double-capstan system is a predictable position controller. The design tradeoffs must be kept in mind when choosing capstan radius, R , initial tension T_L in the strings, mass M of the cart, capstan gain $e^{f\theta}$, and input tensions $\Delta T = KX_{in}$. The best results are obtained when the designer considers

the force required to move the mass, and the magnitude of the input force and displacement available to the input lever. The constraint of straight-line motion limits the application of the controller. It will be useful in situations where small motions must move a large mass easily in a straight path, and the power to the motor driving the capstan is of secondary importance.